ORIGINAL RESEARCH

Surface modification of ramie fibers with silanized CNTs through a simple spray-coating method

Wanru Wang · Guijun Xian · Hui Li

Abstract Preliminary studies performed have indicated that carbon nanotube (CNT) coating is an effective method to enhance the bonding between a natural fiber and a resin matrix. However, the reported coating process is complex, and the improvement of the bonding strength is limited owing to obvious CNT aggregation. This paper reports a simple spray-coating method with uniform distribution of CNTs coated on ramie fiber surfaces. The dispersion of CNTs in a suspension for spray-coating was found to play a key role in CNTs distribution on the fiber surface. Silylated CNTs can be stably and uniformly suspended in a water and alcohol solution with a polyvinylpyrrolidone dispersant. The suspension was sprayed onto ramie fabric by using a hand-spraying pot, and CNTs were distributed on the fiber surface uniformly, as indicated by scanning electron microscopy results. The agglomeration of CNTs on the fiber surface became increasingly evident with an increase in the number of spray layers (from one to six). The effects of CNT coating on the flexural properties of the related composite and bonding properties were studied. The CNT-coated ramie fiber reinforced epoxy plate was prepared by a vacuum assistant resin transfer molding method. The CNT coating increased the flexural strength and modulus of the composite by 38.4% and

36.8%, respectively. A microdebonding test showed that the CNT coating increased the interfacial shear strength between a single ramie fiber and the epoxy resin by 25.7%, which is believed to result from stronger mechanical interlocking and chemical bonding.

Keywords Ramie fiber · Surface modification · CNT · Mechanical properties · Interfacial shear strength

Introduction

Natural fiber-reinforced polymer composites (NFRPs) have recently found widespread applications in engineering because of their satisfactory mechanical properties and low environmental impact (Li et al. 2018; Zhou et al. 2014b). Among various plant fibers used for composite reinforcements, ramie fibers have been studied extensively as a high-potential material for NFRP applications as they possess superior mechanical properties (Faruk et al. 2012; Gurunathan et al. 2015; Yan et al. 2014).

In contrast to conventional synthetic fiber-reinforced polymer composites (examples of such fibers are glass fiber and carbon fiber) (Li et al. 2019; Wang et al. 2018), NFRPs possess some disadvantages for engineering applications, such as poor hydrothermal resistance and poor mechanical properties, as well as

W. Wang · G. Xian (✉) · H. Li
School of Civil Engineering, Harbin Institute of Technology (HIT), 150090, Harbin, China
e-mail: gjxian@hit.edu.cn

high variation in these properties. These problems mainly arise from the characteristics of natural fibers, such as the presence of numerous hydroxyl groups, complex geometry, and defects on the fiber surfaces (Wang et al. 2015). Hence, methods for physical or chemical surface modification are widely adopted to enhance the natural fiber–resin bonding and to reduce the hydrophilicity of the fibers (George et al. 2016; Pickering et al. 2016).

One of the most common treatment methods for natural fibers is alkaline treatment (Orue et al. 2016). Through alkaline treatment, low molecules such as hemicellulose, lignin, and wax are removed to some extent and the roughness of the natural fibers is enhanced, benefiting the adhesion between the fiber and resin. Silane treatment (Xie et al. 2010; Zhou et al. 2014a) and chemical grafting (Amiri et al. 2015) result in some long chemical chains on the fiber surfces, which may react with the resin matrix to form strong covalent bonds. The treated fiber-reinforced NFRPs are reported to significantly enhance the mechanical properties and hydrothermal resistance (Dittenber and GangaRao 2012).

In recent years, nanoparticles (e.g., graphene, carbon nanotube (CNT), nanoclay, TiO_2, and Cu) have been coated onto natural fiber surfaces to enhance adhesion to a resin matrix (Lakshmanan and Chakraborty 2017; Lefatshe et al. 2017; Raabe et al. 2014; Rytlewski et al. 2018; Sarker et al. 2018; Wang et al. 2017). For example, TiO_2 particles were grafted onto flax fibers by the immersion of flax fiber fabric in a TiO_2 suspension under ultrasonication (Wang et al. 2015). However, this method results in the agglomeration, rather than uniform distribution, of the grafted TiO_2 particles. The grafting of TiO_2 on a flax fiber surface significantly increases both the tensile strength of the fibers and the interfacial shear strength between the flax fiber and the epoxy resin. In addition, a functionalized Cu nanoparticle suspension was applied to saturated unidirectional flax natural fibers, whose surfaces were previously tailored with the cationic agent triethylammonium chloride (Sherief et al. 2017). Nanometer-sized Cu particles were grafted on the flax fibers, and a remarkable improvement of 75% in the tensile strength and 50% of the modulus for the treated flax fibers was reported. Hydrous ZrO_2 nanoparticles produced by the hydrolysis of zirconium oxychloride solution was grafted onto flax fiber yarns, and a remarkable increase in the fiber–resin bond strength

was found (Ajith et al. 2016). As reported recently (Sarker et al. 2018), graphene oxide and graphene flakes were coated onto jute fibers, similar to the abovementioned TiO_2 grafting, and both the tensile properties of the fiber and the fiber–resin adhesion were significantly enhanced. Stronger mechanical interlocking and possible chemical bonds owing to nanoparticle treatment are believed to enhance the fiber–resin bonding properties (Sarker et al. 2018; Wang et al. 2015).

CNTs, which possess a naturally high aspect ratio and excellent mechanical properties, are considered to have a great potential in modifying fiber–resin interfacial bonding. CNT grafting on carbon fibers has been reported to successfully enhance the interface strength of carbon–fiber–resin matrix (Deng et al. 2018). However, research on CNT grafting on natural fibers has been scarce. Li et al. (2014) used a "soaking and spray-drying" process to coat COOH–CNTs onto flax fibers. CNT particles were confirmed to disperse on the flax fiber surface through scanning electron microscopy (SEM) analysis. The maximum enhancements of the interfacial shear strength, mode-I interlaminar fracture toughness, and interlaminar shear strength were 26%, 31%, and 20%, respectively.

In summary, grafting of nanometer-sized material can be considered as a novel method to treat natural fibers for improved fiber–resin bonding properties and mechanical properties of NFRP. However, most grafting methods are complicated and time-consuming, and generally, the nanometer-sized materials aggregate on the fiber surfaces. A study on carbon fiber–epoxy bonding indicated that agglomeration of the grafted CNTs leads to an insufficient enhancing effect (He et al. 2007).

This paper aims to propose a simple spray method to realize CNT coating on a ramie fiber surface. In addition, CNTs are modified using surface functional methods to reduce or eliminate CNT agglomeration in the suspension and on the coated fiber surfaces. Finally, the effects of CNT coating on the bonding between ramie fiber and resin, and the mechanical properties of a ramie fabric-epoxy composite plate are studied. This study provides a novel natural fiber surface modification method to realize the high performance of natural fibers based on composites.

Experimental

Raw materials

Ramie fabric provided by the Beijing Institute of Aeronautical Materials, Beijing, China, is categorized as bidirectional ramie fabric. The width is 1000 ± 10 mm, and the surface density is 140 ± 5 g/m^2.

The epoxy resin (bisphenol-A, DGEBA) with a room-temperature-curable agent have a weight ratio of 100:34. The diameter of hydroxylated multiwalled CNT is 20–30 nm, the length is 10–50 μm, and the purity is 98 wt%. The -OH content is 1.76%.

A KH550 silane coupling agent (γ-amino-propyltriethoxysilane) is used, and its molecular formula is $H_2NCH_2CH_2CH_2Si(OC_2H_5)_3$. Two dispersants are used in the present study, i.e., polyvinylpyrrolidone (PVP) and sodium dodecyl benzene sulfonate (SDBS).

Ramie fabric treatment

In the present study, the ramie fabric was treated with an alkaline solution, and a silane coupling agent was spray coated with CNT suspension. Each treatment is described below.

Control treatment: the ramie fabric was immersed in distilled water at 60 °C under ultrasonication (Ultrasonic cleaning machine, Model G-060 s, 40 Hz) for 30 min. The treated fabric was then dried in an oven at 110 °C for 2 h. The fabric is designated as "C."

Alkaline solution treatment: the ramie fabric was immersed in 5.0 wt% NaOH solution at 60 °C under ultrasonication for 15 min. After that, the fabric was rinsed with distilled water until the pH value reached 7. The treated fabric was then dried in an oven at 110 °C for 2 h, and designated as "A."

Silane coupling treatment: the ramie fabric was first treated with an alkaline solution, as mentioned above, and then immersed in a silane coupling solution at 60 °C for 30 min. After that, the fabric was dried in an oven at 110 °C for 2 h, and the fabric was designated as "S." To prepare the silane coupling solution (the two pictures on the left in Fig. 1), 2 wt% silane coupling agent was added to a mixture of ethanol and water solution (weight ratio of 9:1) and magnetically stirred for 20 min at room temperature.

CNT suspension spray: for the ramie fabric coated with CNT suspensions, the first step was to prepare a CNT suspension. The CNT suspension was then spray-coated onto the ramie fabric using a hand spray pot. Three kinds of CNT suspensions were prepared. There are three steps for the preparation of a suspension, as presented below.

1. Figure 1 shows the preparation routine for a CNT suspension (including the preparation of the silane coupling solution). 0.5 wt% CNTs were slowly added to the prepared silane coupling solution at room temperature and magnetically stirred for 10 min. Next, 0.5 wt% PVP was mixed into the above CNT suspension and sonicated for 10 min at room temperature. Then, the obtained suspension was kept at 60 °C for 4 h. Afterwards, the suspension was cooled down to room temperature and will be used as a spray coating. It was named "P-CNT."

2. The preparation routine is the same as the first one. However, the dispersant of 0.5 wt% PVP was changed to 0.5 wt% SDBS. It was designated as "S-CNT."

3. Similar to the first routine, no dispersant was added. The suspension was designated as "C-CNT."

Spray coating was performed using a hand-spray pot. The ramie fabric for spray coating was alkaline-treated as per the aforementioned procedure. The sprayed fabric was then kept for 0.5 h at room temperature, and the solvent in the suspension was volatilized to some degree. The fabric can be repeatedly spray-coated via this process. Finally, the coated fabric was dried in an oven at 110 °C for 2 h and was designated as "CNT." The amount of CNT coated onto the ramie fabric surface in one layer of the coating was about 2 g/m^2 (Fig. 2). The fabric was suspended and spray-coated uniformly on both sides by hand, as shown in Fig. 3. It is worth noting to avoid spillage of CNTs during the spray coating, a spray box was used as shown in Fig. 3. The box was covered with transparent plastic film and the spray coating was performed inside.
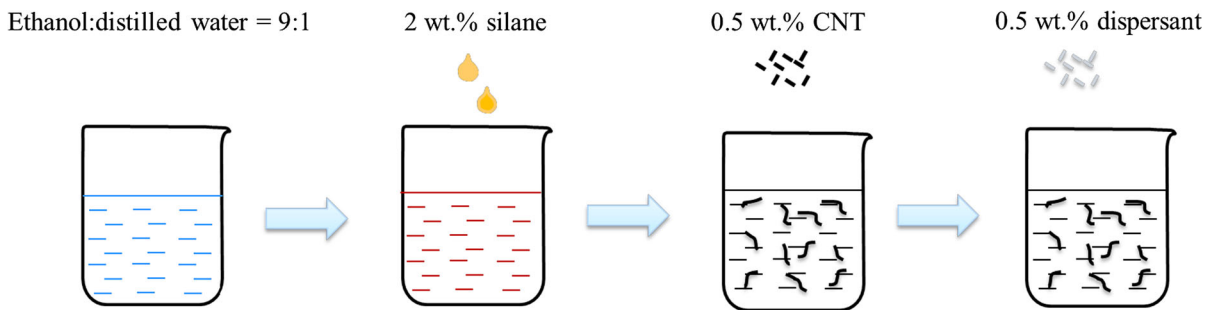
Ethanol:distilled water = 9:1   2 wt.% silane   0.5 wt.% CNT   0.5 wt.% dispersant

Fig. 1 Preparation routine for CNT suspensions

CNT suspension

Before every repeat spraying
keep in RT for 0.5 h

110℃ for 2 h

Spraying both sides
2 g/m² per layer of CNT coating

Ramie fabric
coated with CNT
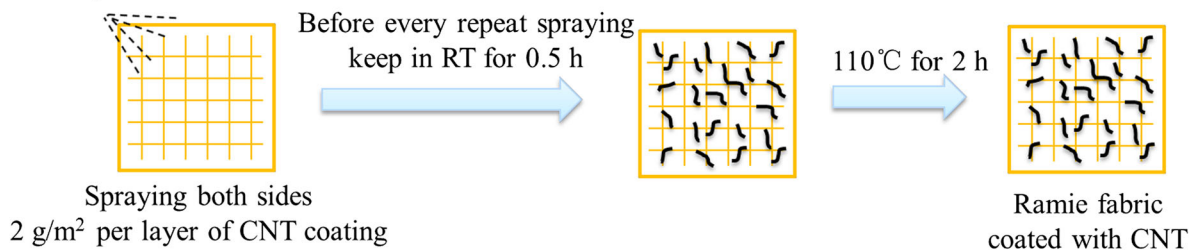
Fig. 2 Schematic sketch of spray coating process with CNT suspensions onto ramie fabric

Spray box   Spray pot   C   A   S   2 layers 4 layers 6 layers

Fig. 3 Photographs of a spray box, a hand spray pot and treated ramie fabrics

Preparation of ramie fabric-reinforced epoxy plate (RREP)

RREPs were prepared using a vacuum-assisted resin transfer molding process (Fig. 4). Each plate was made of eight layers of ramie fabric. The impregnated fabric plate was cured at room temperature for 2 days and then post-cured in an oven at 110 °C for 2 h. The thickness of the fabricated plate was 2.03–2.15 mm.

SEM analysis

SEM was used to observe the morphology of ramie fibers, and the test voltage was set as 5 kV. A conductive adhesive was used to stick ramie fibers on an aluminum sheet, and the fiber surface was coated with a layer of gold for 15 min by using a precision etching and plating instrument.
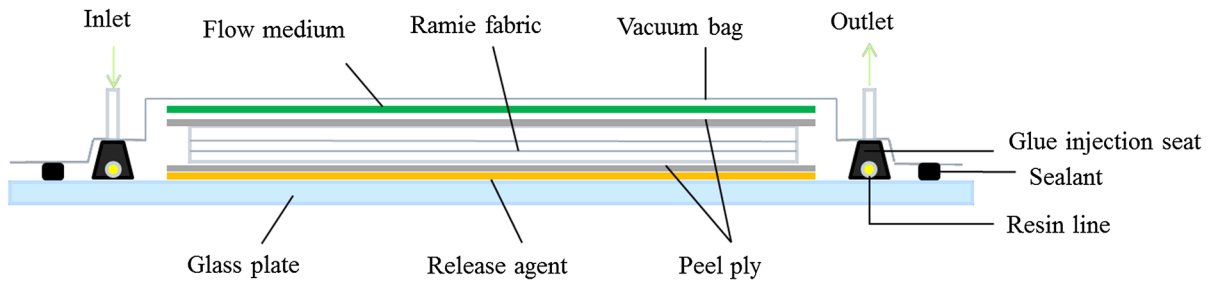
Fig. 4 Sketch of vacuum-assisted resin transfer molding (VARTM)

Three-point bending test

A three-point bending test was conducted on the RREP using a tensile machine, according to ASTM D790 (2003). The thickness of the sample was in the range of 2.03–2.15 mm, and the width and length were cut to 13 and 80 mm, respectively. The tests were conducted under 50% humidity at room temperature. Five measurements were recorded for each group, and the average value was reported.

Microbond pull-out test of ramie fiber/epoxy resin

First, a yarn was taken from the ramie fabric. Then, an elementary fiber was carefully extracted from the yarn. Resin droplets were deposited onto the elementary fiber, which is similar to the preparation of droplet on a carbon filament (Wang et al. 2016). The diameter of the resin droplets ranged from 150 to 200 μm. The sample was cured in an oven at 60 °C for 11 h and at 110 °C for another 2 h.

A microbond pull-out test (tester Model HM410, Japan Tung Lung Co., Ltd., Japan) was performed to determine the interfacial shear strength. For each kind of sample, at least 20 tests were performed. The test speed was set as 0.1 mm/min.

Three types of samples were prepared. The first was a control fiber, which was defined as "C." The second was fiber sprayed with three coating layers of P-CNT, which was defined as "CNT." The third was fiber sprayed with three coating layers of P-CNT and then washed with distilled water ultrasonically (60 °C, 40 Hz). This sample was labeled "U-CNT."

Results and discussion

The present paper aims to develop a simple spray-coating method to graft CNTs onto natural fiber fabric with CNT suspensions. It is considered that the stable and uniform dispersion of CNTs in the suspension will play a key role in the distribution of CNTs on the fiber surfaces. Therefore, the present work first attempted to obtain a stable, well-dispersed CNT suspension with appropriate dispersants. Subsequently, the morphology of CNTs on the suspension-coated fiber surfaces and the effects of the grafted CNTs on the mechanical properties of the RREPs were investigated.

CNT suspensions for spray coating

Three types of 0.5 wt% CNT suspensions were prepared in the present study (Fig. 1). The CNTs were first treated with a silane coupling agent and then dispersed into a mixture of ethanol and water solution with or without dispersant. The suspensions were kept in the laboratory for some time to check if the CNTs
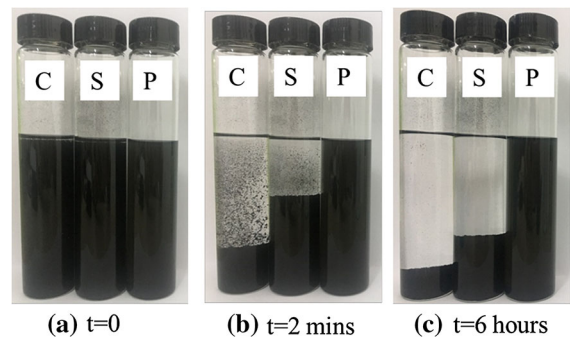

(a) t=0   **(b)** t=2 mins   **(c)** t=6 hours

Fig. 5 Photographs of 0.5 wt% CNT suspension as a function of time: **a** 0 min, **b** 2 min, and **c** 6 h with a dispersant of PVP (P-CNT), SDBS (S-CNT) or without dispersant (C-CNT)

were stable for a prolonged period. As shown in Fig. 5, without dispersant, CNTs tend to settle down in a very short time (e.g., less than 2 min of standing) in the suspension. It is well-known that the agglomeration of CNTs tends to occur owing to the van der Waals force between CNTs (Wang et al. 2014). Note that CNTs for the suspension with SDBS, PVP, and without dispersants (S-CNT, P-CNT, and C-CNT) were treated with the silane coupling agent.

As reported, silane-coupling-treated CNTs can be stably dispersed in an ethanol suspension without deposition (Ma et al. 2006). However, in the present study, a contrasting phenomenon was found for C-CNT. Although to some degree silane molecules can enhance the hydrophilicity of CNT surfaces by forming covalent bonds with the CNT surface, as believed, the limited number of active sites on the CNT surface may limit the effectiveness of the dispersity (Geng et al. 2008; Ma et al. 2007). This is owing to the limited hydroxide radicals of the CNT surface. Because of the reaction between silane molecules and CNT, the dispersity can improve only within a certain range.

Compared to the suspension without dispersant, the addition of dispersants of SDSB or PVP benefits the stability of the dispersion of CNTs (Fig. 5). Nevertheless, with SDSB, the agglomeration of CNT still occurred to a relatively lower extent compared to the case of C-CNT, even only after 2 min of standing. As indicated, CNTs can be well dispersed in water using anionic surfactant, which possesses both hydrophilic polar groups and hydrophobic lipid chains (Sahoo et al. 2010). The hydrophobic lipid chain attaches to the surfaces of CNTs, while the hydrophilic side can disperse in the polar media. However, compared with PVP, SDBS showed weaker dispersity because of the weaker interaction with CNTs (Sahoo et al. 2010).

PVP exhibited an excellent effect on the stabilization of the dispersed CNTs. After 6 h of standing, no hints of agglomeration of CNTs were found (Fig. 5). As a water-soluble polymer, PVP can increase the solubility of CNTs in an aqueous solution through a physical association that can be explained by a wrapping mechanism (Bravo-Sanchez et al. 2010; Kim et al. 2012; Yadav and Singh 2016). PVP modules can be adsorbed onto the CNT surface and form to the supermolecule. The steric hindrance effect of supermolecule can prevent the agglomeration of CNTs by decreasing the surface tension and

overcoming the van der Waals force between CNTs (Wang et al. 2014).

In summary, PVP was considered as an effective dispersant and can help realize a stable dispersion of CNTs in a mixture of ethanol and water solution.

CNT distribution on ramie fabric through spray coating

Using a hand spray pot, ramie fabrics were sprayed with the abovementioned CNT suspensions on both sides. After drying in an oven at 110 °C for 2 h (Fig. 2), the fabrics were cut and analyzed with SEM (Fig. 6).

Figure 6a–d presents the SEM images of ramie fibers treated with alkali only (Fig. 6a), one layer of spray coating of C-CNT (Fig. 6b), one layer of spray coating of S-CNT (Fig. 6c), and one layer of spray coating of P-CNT (Fig. 6d). Figure 6e, f show the ramie fiber with three and six layers of spray coatings of P-CNT, respectively.

As found in Fig. 6b–d, CNTs were coated onto the ramie fiber surfaces. In addition, heavy aggregation is seen in Fig. 6b, c for the suspensions of C-CNT and S-CNT, while very uniform distribution of CNTs on the fiber surfaces is found for the suspension of P-CNTs (Fig. 6d). Accordingly, it can be concluded that CNTs can be coated onto ramie fiber surfaces through a simple spray-coating method using a hand-spraying pot. In addition, the distribution of CNTs on the fiber surfaces is related to the fiber dispersion in the suspensions. CNTs were stably and uniformly dispersed inside the suspension (P-CNT) with the assistance of PVP. Through the spray process, CNTs were uniformly distributed onto the fiber surfaces. However, the aggregation of CNTs in C- and S-CNT suspensions is expected not to change through the simple spray process, and CNTs will exhibit aggregation on the coated fiber surfaces (Fig. 6b, c). The addition of SDSB is somewhat beneficial for the dispersion of CNTs in the suspension, as indicated in the above section, which leads to a slightly better distribution of CNTs on the fiber surfaces.

Figure 6d–f present the effects of spray layers on the CNT morphology of the fiber surfaces with the P-CNT suspension. With an increase in the number of spray layers from 1 to 3 and then to 6, the aggregation of CNTs on the fiber surface became more significant. It is worth noting that unlike one layer of coating
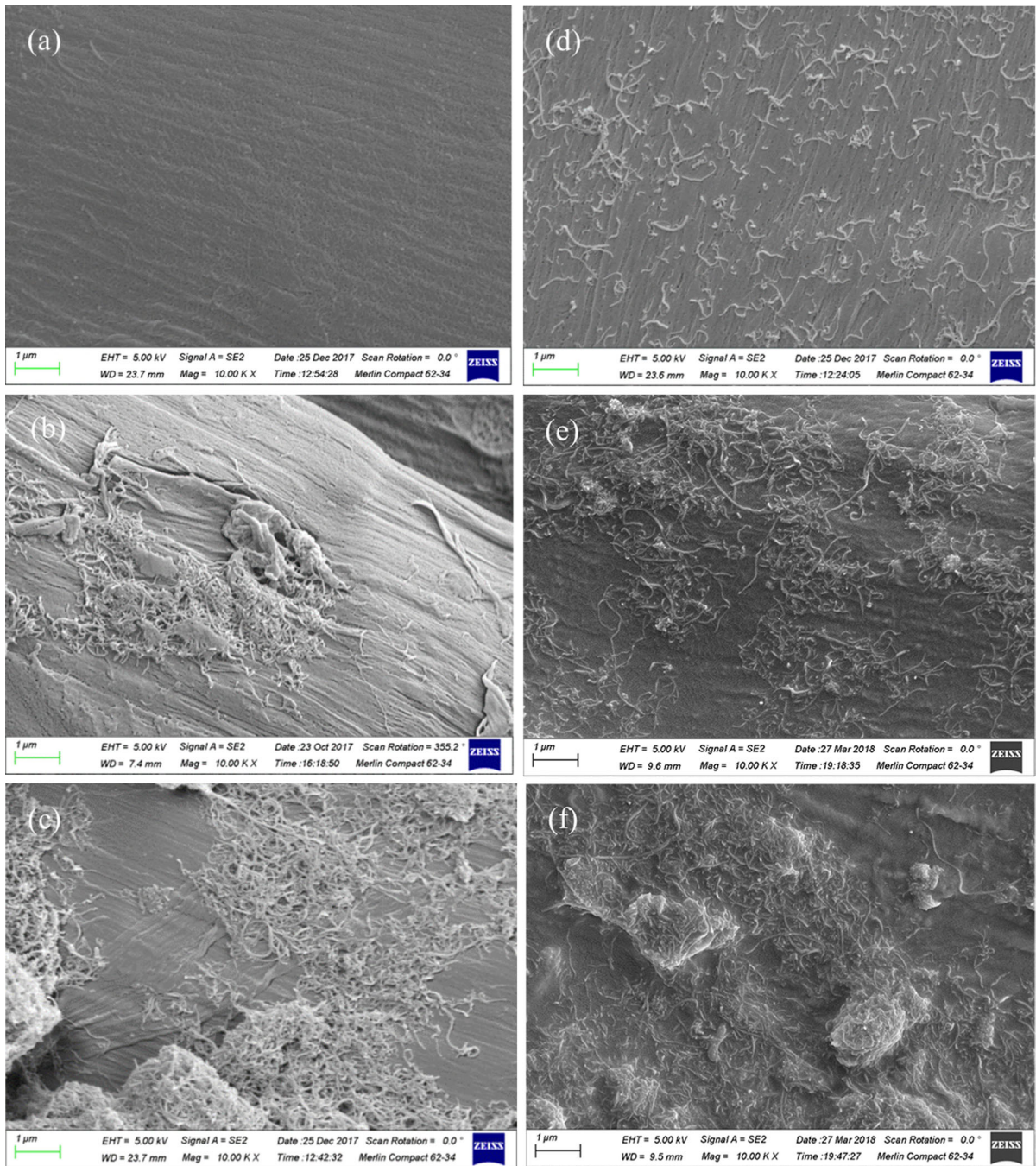
Fig. 6 SEM images of **a** alkali fiber, **b** one coating layer of C-CNT, **c** one coating layer of S-CNT, **d** one coating layer of P-CNT, **e** three coating layers of P-CNT, and **f** six coating layers of P-CNT

(Fig. 6d), CNTs on fiber surfaces in more spraying layers tend to aggregate in several tens of microns, with some space without CNTs (Fig. 6e, f). This is attributed to the spray coating process. For more spray layers, after one layer of spray, the fabric will be sprayed with another layer after drying in air at room temperature for 30 min. During the first spray, the liquid of the suspension can be quickly absorbed by

the ramie fibers, and only CNT was left on the surfaces uniformly. During the following spray, because the fiber is saturated with the suspension, the suspension sprayed onto the fiber surface will need more time to evaporate. The flow of suspension may occur during this period, resulting in the aggregation of CNTs as found in Fig. 6e, f.

In addition, the silane coupling agents remain on the fiber surfaces rather than penetrating the fiber, as demonstrated by the SEM images shown in Fig. 6e, f. CNTs were covered by a film rather than simply being attached to the fiber surfaces (Fig. 6d). The film can be washed out ultrasonically with distilled water (Fig. 7). In addition, after washing, the grooves of the fibers were clearly presented. Compared with the control fiber, the film is considered a silane coupling agent that did not completely react.

Comparing Figs. 6e and 7, CNTs on the fiber surfaces do not seem to be removed completely by the washing process. This indicates that the coated CNTs may be covalently bonded to the fiber surfaces rather than through a weak van der Waals force. The washing process is schematically shown in Fig. 8a, b.

The formation of covalent bonds between CNTs and the ramie fiber surface is attributed to the function of the silane coupling agents. As mentioned above, CNTs were pretreated with silane coupling agents before being added to the suspension (Fig. 1). The silane molecule chain reacted with the hydroxyl groups of ramie fibers through Si–O–C covalent bonds (Sandler et al. 1999). Heating can also promote the condensation of free silanol groups, forming solid
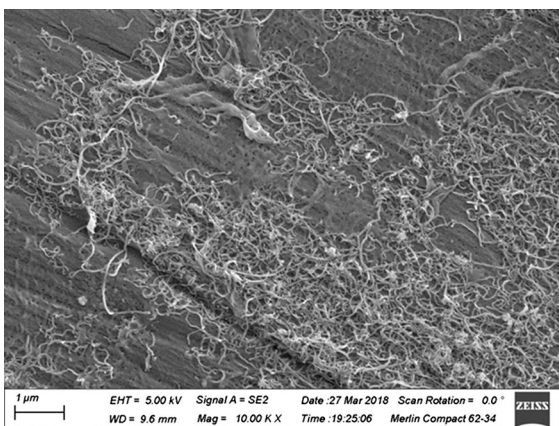
polysiloxane networks in the cell walls. Hydrogen bonds can also form between the Si–O–Si backbone and the hydroxyl groups of fibers. Figure 8c schematically shows the possible bond mechanisms. With regard to the fast evaporation of solvent, only a thin layer of silane coupling agent can react with the fiber surfaces and CNTs.

To elucidate the effects of the silane treatment of CNTs on the bonding between CNTs and ramie fibers, a comparative test was conducted using a suspension similar to P-CNT. One difference was that the CNTs were not treated with silane treatment. Figure 9a, b show SEM images of the ramie fibers when spray coated with the suspension with untreated CNTs. The agglomeration of CNTs on the fiber surfaces is obvious (Fig. 9a), indicating that the dispersion of untreated CNTs even with PVP dispersant cannot be uniform or stable. The silane treatment of CNTs is also a key factor in realizing the stable and uniform dispersion of CNTs in suspensions. After washing ultrasonically, the coated CNTs on the fiber surfaces were almost completely removed. This indicates that the bonding between CNTs (without silane treatment) and ramie fiber may only result from a weak van der Waals force.

Mechanical properties of composites

CNT coating is more effective than traditional fiber-surface-modification methods. As the result of three-point bending test, alkali treatment increased the bending strength and modulus of RFRP by 7.5% and 1.4%, respectively. The silane coupling agent treatment increased the strength and modulus by 9.0% and 6.1%, respectively. As shown in Fig. 10, the ramie fiber coated with CNT increased the three-point bending strength and modulus of the composite plates by 38.4% and 36.8%, respectively. The three-point bending property reflects the macroscopic interface property of the composite, which shows that the interfacial bonding performance of the composites significantly improved after the coating treatment of CNT.

The improvement in the mechanical performance is mainly attributed to adsorption, infiltration, chemical bond cooperation, and mechanical engagement (Orue et al. 2016). Alkali treatment can remove small molecules on the fiber surface and improve the roughness of the fiber surface, which can enhance
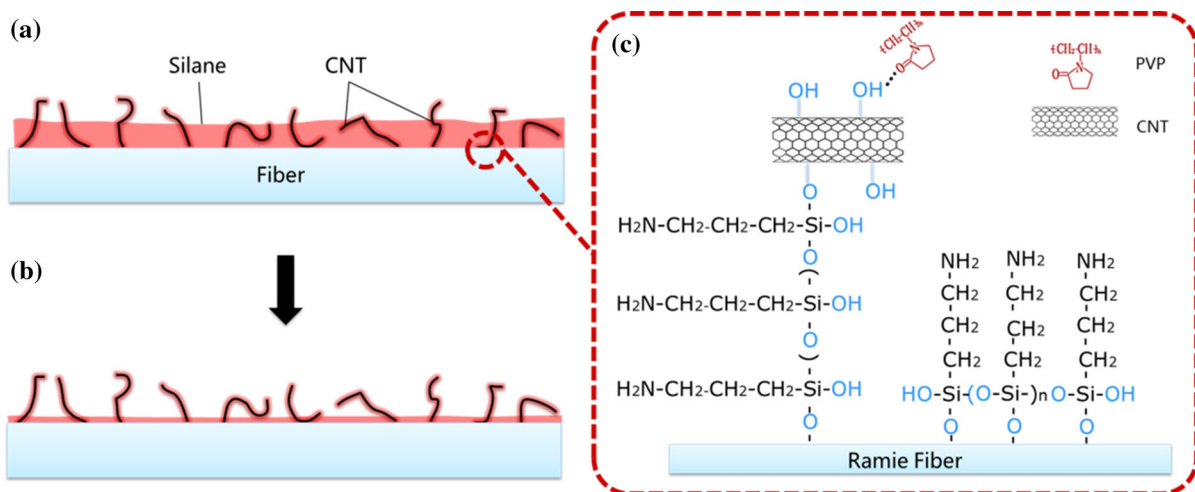

Fig. 7 SEM image of three coating layers of P-CNT after ultrasonic washing

Fig. 8 Schematic of **a** ramie fiber coated with P-CNT, **b** P-CNT ramie fiber after ultrasonic washing, and **c** molecular structure of fiber surface reacted with silanized CNT and silane
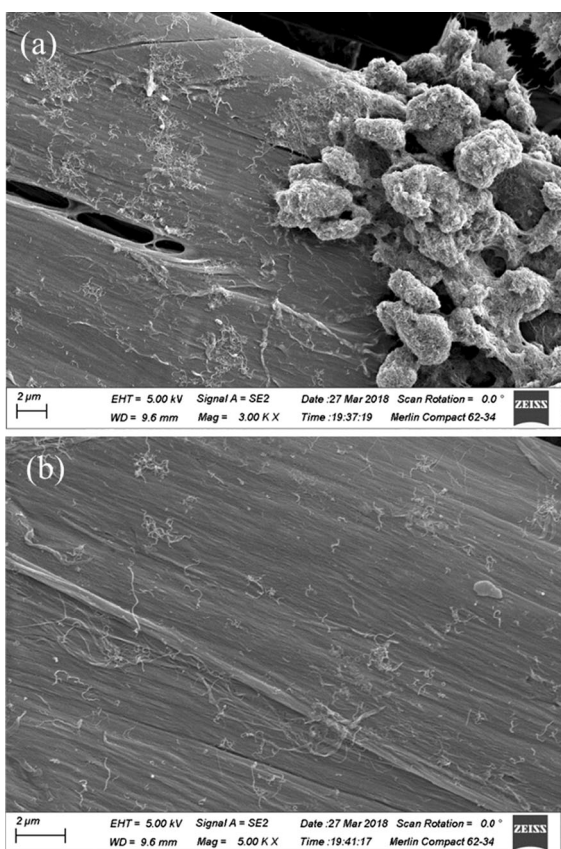

Fig. 9 SEM images of three-coating-layer suspension: **a** CNT containing PVP only and **b** CNT containing PVP after ultrasonic washing
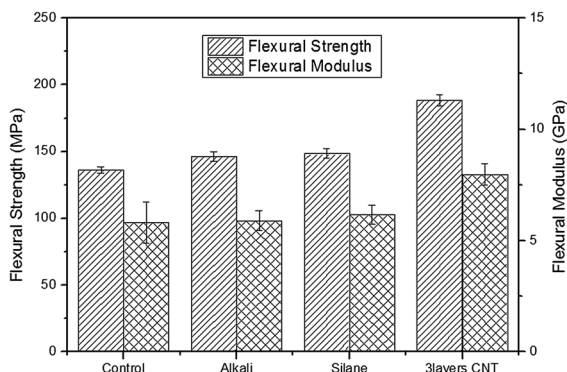

Fig. 10 Flexural properties of RREP for different treatments

the mechanical interaction between fiber and resin (Kumar Sinha et al. 2017; Sullins et al. 2017; Yu et al. 2010). The coupling agent can form new chemical bonds between the fiber and the resin (Yu et al. 2010, 2014; Zhou et al. 2014a). The silane coupling agent reacted with the hydroxyl groups on the surface of the ramie fiber to form a thin film. In addition, a coupling agent can improve the infiltration between fiber and resin, but limited information is available on this mechanism. After coating with P-CNT, the roughness of the fiber surface improved, and the chemical bonds between fiber and resin increased the interfacial strength. At the same time, the one-dimensional CNT prevented the propagation of cracks. These helped to improve the bending properties of the composite.

The coating amount and dispersal state of CNTs had a significant influence on the effect of interface modifications. By comparing the effects of spraying time on the bending properties of ramie fiber composites, the optimum coating amount of CNT on the fiber surface was determined. Figure 11 shows the effect of CNT content on the flexural properties of composites. When three layers of suspension were sprayed, the flexural strength and modulus of the composite increased the most by 38.4% and 36.8%, respectively. After more than three layers, the flexural performance began to decline with the increase in the number of coating layers. With an increase in the spraying time, CNTs accumulated on the fiber surface. This was equivalent to a high concentration of CNT coated on the fiber surface. A large number of agglomerated CNTs were loose in the structure and could not effectively transfer the resin stress to the fibers. This is the main reason for the deterioration of mechanical properties caused by excessive spraying times.

Based on the above-mentioned studies, when three layers of CNT suspension were sprayed, the bending performance of the fiber composites showed the most significant improvement. On the basis of the three layers of suspension, the effect of CNTs on the adhesion performance of the fiber–resin interface will be further analyzed on the mesoscale.

As shown in Fig. 12, the shear strength of the interface before and after washing was tested by performing a microbond test. Compared with untreated samples, the interfacial shear strength increased by 25.7% after coating with three layers of CNT and 36.0% after ultrasonic washing. A surface
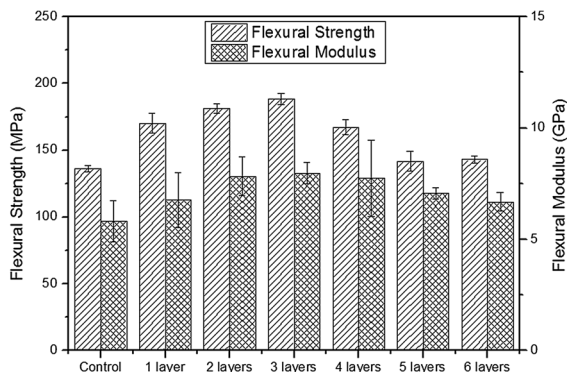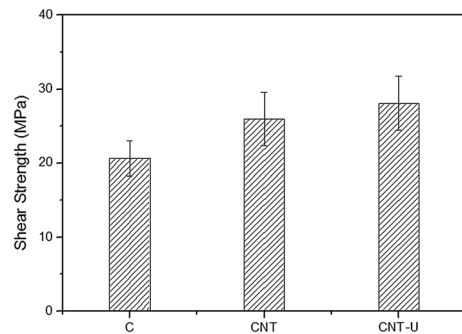

Fig. 12 Shear strength of microbond tests for different P-CNT treatments

coating of CNTs can effectively improve the interfacial bond performance. These results show that ultrasonic washing can further enhance the shear strength of the interface.

As mentioned previously, the sprayed CNT is in the covering layer of the silane coupling agent. Although the coating layer can improve the coating strength of CNTs on the fiber surface, a too-thick unreacted silane coupling agent layer can limit the contact area between the CNTs and resin (Xie et al. 2010). The unreacted silane coupling agent film can be removed by ultrasonic washing, as shown in Fig. 8b. After washing with ultrasonic waves, the coating state between the CNTs and fiber was still sufficient. However, the contact area between the resin and CNTs can be expanded, which leads to an obvious enhancement in the mechanical lock cooperation between the resin and the fiber, as shown in Fig. 15.

The interfacial bonding between untreated ramie fiber and resin is poor. Figure 13a shows the debonding between the control fiber and resin. After debonding, the surface of the control fiber was smooth, and the amount of resin adhesion was low. Part of the surface area of the fibers after the coating treatment of CNT had peeling failures on the fiber surface and a significant amount of resin attached to part of the fiber surface, as shown in Fig. 13b. The above phenomenon indicates that the interfacial bond performance between fiber and resin was significantly improved, and the weak layer of the interfacial area transferred to the interior of the fiber epidermis or matrix (Fig. 14). Compared with carbon fiber, ramie fiber is a kind of natural fiber with a complex cell wall structure (Arnould et al. 2017). When the interfacial shear strength of the fiber and the resin is higher than the
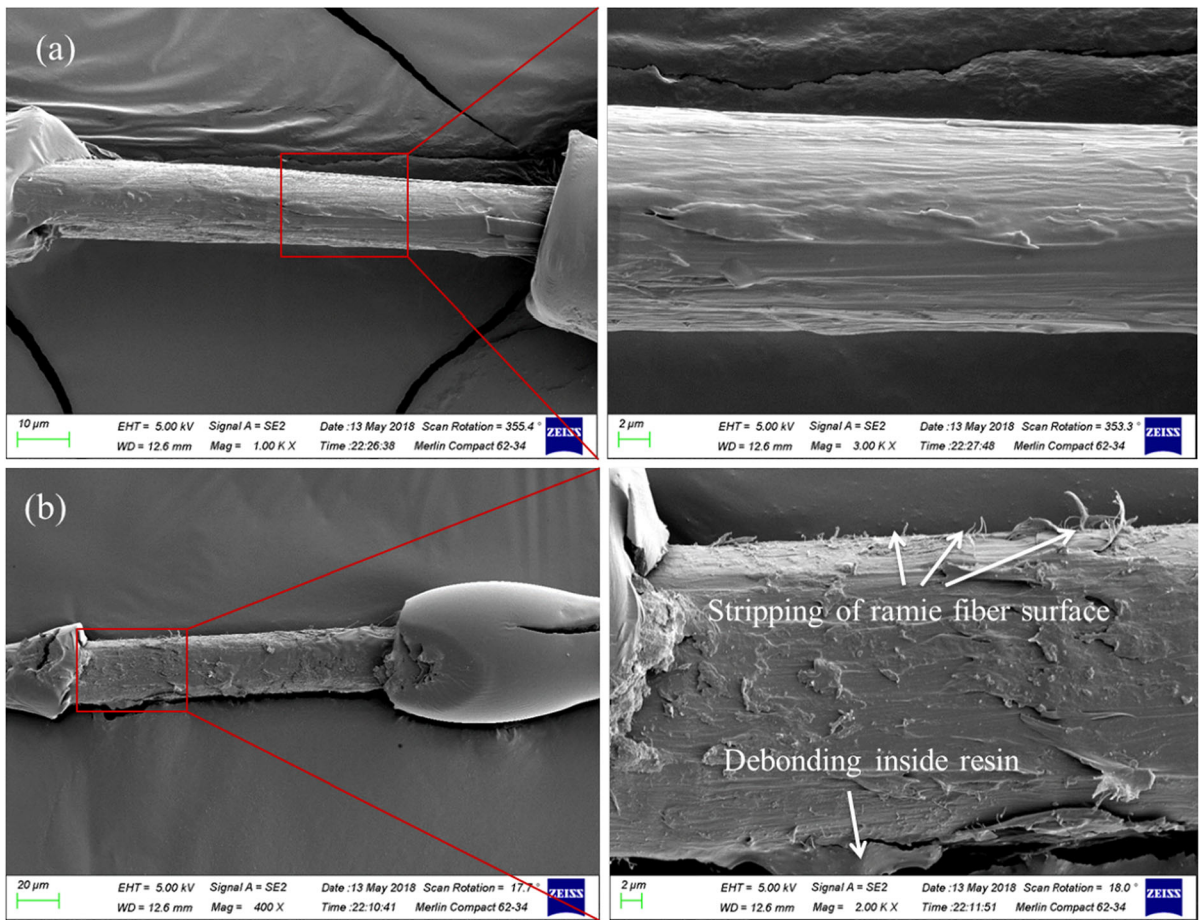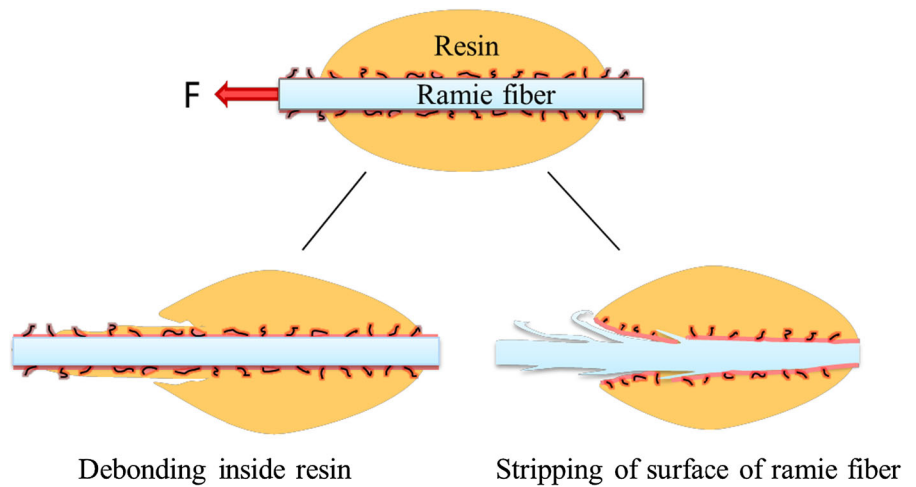

Fig. 11 Flexural properties of RREP for different P-CNT content

Fig. 13 SEM images of **a** control fiber and **b** P-CNT fiber debonded from epoxy resin

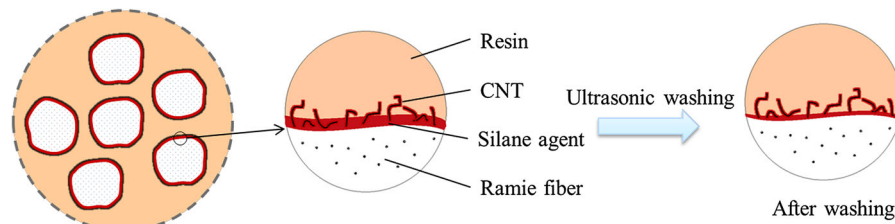**Fig. 14** Schematic diagram of debonding between P-CNT fiber and resin

Fig. 15 Schematic diagram of P-CNT grafted fiber/resin interface

bond strength inside the fiber, peeling failure occurs on the fiber surface. A diagram of the interface debonding is shown in Fig. 15.

Conclusions

A simple spray coating method was proposed to graft CNTs onto ramie fabric. Well-dispersed CNT solution was prepared. The distribution of CNTs on the fiber surface was investigated. In addition, the effect of CNT coating on the flexural properties of a ramie fabric-epoxy composite plate were studied. The following conclusions can be highlighted.

1. A stable and uniformly dispersed and silanized CNT suspension was realized with polyvinyl pyrrolidone (PVP) in a mixture of ethanol and distilled water.
2. Using a hand spray pot, silanized CNTs can be uniformly coated on the fiber surface. The agglomeration of CNTs on the fiber surface became increasingly evident with an increase in the number of spray layers (from one to six layers).
3. The flexural properties and interfacial properties of a ramie fabric-epoxy composite plate can be improved by 38.4% and 36.8%, respectively by using CNT coating. Meanwhile, the CNT coating increased the interfacial shear strength between a single ramie fiber and the epoxy resin by 25.7%.

References

Ajith A, Xian G, Li H, Sherief Z, Thomas S (2016) Surface grafting of flax fibres with hydrous zirconia nanoparticles

and the effects on the tensile and bonding properties. J Compos Mater 50:627–635. https://doi.org/10.1177/0021998315580450

Amiri A, Ulven CA, Huo S (2015) Effect of chemical treatment of flax fiber and resin manipulation on service life of their composites using time–temperature superposition. Polymers 7:1965–1978. https://doi.org/10.3390/polym7101493

Arnould O, Siniscalco D, Bourmaud A, Le Duigou A, Baley C (2017) Better insight into the nano-mechanical properties of flax fibre cell walls. Ind Crops Prod 97:224–228. https://doi.org/10.1016/j.indcrop.2016.12.020

ASTM D790 (2003) Standard test methods for flexural properties of unreinforced and reinforced plastics and electrical insulating materials. American Society for Testing and Materials, West Conshohocken

Bravo-Sanchez M, Simmons TJ, Vidal MA (2010) Liquid crystal behavior of single wall carbon nanotubes. Carbon 48:3531–3542. https://doi.org/10.1016/j.carbon.2010.05.051

Deng Y, Islam MS, Tong L (2018) Effects of grafting strength and density on interfacial shear strength of carbon nanotube grafted carbon fibre reinforced composites. Compos Sci Technol 168:195–202. https://doi.org/10.1016/j.compscitech.2018.09.025

Dittenber DB, GangaRao HVS (2012) Critical review of recent publications on use of natural composites in infrastructure. Compos A Appl Sci Manuf 43:1419–1429. https://doi.org/10.1016/j.compositesa.2011.11.019

Faruk O, Bledzki AK, Fink H-P, Sain M (2012) Biocomposites reinforced with natural fibers: 2000–2010. Prog Polym Sci 37:1552–1596. https://doi.org/10.1016/j.progpolymsci.2012.04.003

Geng Y, Liu MY, Li J, Shi XM, Kim JK (2008) Effects of surfactant treatment on mechanical and electrical properties of CNT/epoxy nanocomposites. Compos A Appl Sci Manuf 39:1876–1883. https://doi.org/10.1016/j.compositesa.2008.09.009

George M, Chae M, Bressler DC (2016) Composite materials with bast fibres: Structural, technical, and environmental properties. Prog Mater Sci 83:1–23. https://doi.org/10.1016/j.pmatsci.2016.04.002

Gurunathan T, Mohanty S, Nayak SK (2015) A review of the recent developments in biocomposites based on natural fibres and their application perspectives. Compos A Appl Sci Manuf 77:1–25. https://doi.org/10.1016/j.compositesa.2015.06.007

He X, Zhang F, Wang R, Liu W (2007) Preparation of a carbon nanotube/carbon fiber multi-scale reinforcement by grafting multi-walled carbon nanotubes onto the fibers. Carbon

45:2559–2563. https://doi.org/10.1016/j.carbon.2007.08.018

Kim SW, Kim T, Kim YS, Choi HS, Lim HJ, Yang SJ, Park CR (2012) Surface modifications for the effective dispersion of carbon nanotubes in solvents and polymers. Carbon 50:3–33. https://doi.org/10.1016/j.carbon.2011.08.011

Kumar Sinha A, Narang HK, Bhattacharya S (2017) Effect of alkali treatment on surface morphology of abaca fibre. Mater Today Proc 4:8993–8996. https://doi.org/10.1016/j.matpr.2017.07.251

Lakshmanan A, Chakraborty S (2017) Coating of silver nanoparticles on jute fibre by in situ synthesis. Cellulose 24:1563–1577. https://doi.org/10.1007/s10570-017-1204-2

Lefatshe K, Muiva CM, Kebaabetswe LP (2017) Extraction of nanocellulose and in situ casting of ZnO/cellulose nanocomposite with enhanced photocatalytic and antibacterial activity. Carbohydr Polym 164:301–308. https://doi.org/10.1016/j.carbpol.2017.02.020

Li Y, Chen C, Xu J, Zhang Z, Yuan B, Huang X (2014) Improved mechanical properties of carbon nanotubes-coated flax fiber reinforced composites. J Mater Sci 50:1117–1128. https://doi.org/10.1007/s10853-014-8668-3

Li Y, Yi X, Yu T, Xian G (2018) An overview of structural-functional-integrated composites based on the hierarchical microstructures of plant fibers. Adv Compos Hybrid Mater 1:231–246. https://doi.org/10.1007/s42114-017-0020-3

Li CG, Xian GJ, Li H (2019) Tension–tension fatigue performance of a large-diameter pultruded carbon/glass hybrid rod. Int J Fatigue 120:141–149

Ma PC, Kim J-K, Tang BZ (2006) Functionalization of carbon nanotubes using a silane coupling agent. Carbon 44:3232–3238. https://doi.org/10.1016/j.carbon.2006.06.032

Ma PC, Kim J-K, Tang BZ (2007) Effects of silane functionalization on the properties of carbon nanotube/epoxy nanocomposites. Compos Sci Technol 67:2965–2972. https://doi.org/10.1016/j.compscitech.2007.05.006

Orue A, Jauregi A, Unsuain U, Labidi J, Eceiza A, Arbelaiz A (2016) The effect of alkaline and silane treatments on mechanical properties and breakage of sisal fibers and poly(lactic acid)/sisal fiber composites. Compos Part A Appl Sci Manuf 84:186–195. https://doi.org/10.1016/j.compositesa.2016.01.021

Pickering KL, Efendy MGA, Le TM (2016) A review of recent developments in natural fibre composites and their mechanical performance. Compos A Appl Sci Manuf 83:98–112. https://doi.org/10.1016/j.compositesa.2015.08.038

Raabe J, de Souza Fonseca A, Bufalino L, Ribeiro C, Martins MA, Marconcini JM, Tonoli GH (2014) Evaluation of reaction factors for deposition of silica (SiO$_2$) nanoparticles on cellulose fibers. Carbohydr Polym 114:424–431. https://doi.org/10.1016/j.carbpol.2014.08.042

Rytlewski P, Stepczyńska M, Gohs U, Malinowski R, Budner B, Żenkiewicz M (2018) Flax fibres reinforced polylactide modified by ionizing radiation. Ind Crops Prod 112:716–723. https://doi.org/10.1016/j.indcrop.2018.01.004

Sahoo NG, Rana S, Cho JW, Li L, Chan SH (2010) Polymer nanocomposites based on functionalized carbon nanotubes. Prog Polym Sci 35:837–867. https://doi.org/10.1016/j.progpolymsci.2010.03.002

Sandler J, Shaffer MSP, Prasse T, Bauhofer W, Schulte K, Windle AH (1999) Development of a dispersion process for carbon nanotubes in an epoxy matrix and the resulting electrical properties. Polymer 40:5967–5971. https://doi.org/10.1016/S0032-3861(99)00166-4

Sarker F, Karim N, Afroj S, Koncherry V, Novoselov KS, Potluri P (2018) High-performance graphene-based natural fiber composites. Acs Appl Mater Interfaces 10:34502–34512. https://doi.org/10.1021/acsami.8b13018

Sherief Z, Xian G, Thomas S, Ajith A (2017) Effects of surface grafting of copper nanoparticles on the tensile and bonding properties of flax fibers. Sci Eng Compos Mater 24:651–660. https://doi.org/10.1515/secm-2014-0462

Sullins T, Pillay S, Komus A, Ning H (2017) Hemp fiber reinforced polypropylene composites: the effects of material treatments. Compos B Eng 114:15–22. https://doi.org/10.1016/j.compositesb.2017.02.001

Wang B, Liu S, Zhu Y, Ge S (2014) Influence of polyvinyl pyrrolidone on the dispersion of multi-walled carbon nanotubes in aqueous solution. Russ J Phys Chem A 88:2385–2390. https://doi.org/10.1134/s0036024414130020

Wang H, Xian G, Li H (2015) Grafting of nano-TiO$_2$ onto flax fibers and the enhancement of the mechanical properties of the flax fiber and flax fiber/epoxy composite. Compos Part A Appl Sci Manuf 76:172–180. https://doi.org/10.1016/j.compositesa.2015.05.027

Wang Z, Huang XY, Xian GJ, Li H (2016) Effects of surface treatment of carbon fiber: tensile property, surface characteristics, and bonding to epoxy. Polym Compos 37:2921–2932

Wang C, Wang S, Cheng H, Xian Y, Zhang S (2017) Mechanical properties and prediction for nanocalcium carbonate-treated bamboo fiber/high-density polyethylene composites. J Mater Sci 52:11482–11495. https://doi.org/10.1007/s10853-017-1285-1

Wang ZK, Zhao XL, Xian GJ, Wu G, Raman RKS, Al-Saadi S (2018) Effect of sustained load and seawater and sea sand concrete environment on durability of basalt- and glass-fibre reinforced polymer (B/GFRP) bars. Corros Sci 138:200–218. https://doi.org/10.1016/j.corsci.2018.04.002

Xie Y, Hill CAS, Xiao Z, Militz H, Mai C (2010) Silane coupling agents used for natural fiber/polymer composites: a review. Compos A Appl Sci Manuf 41:806–819. https://doi.org/10.1016/j.compositesa.2010.03.005

Yadav SP, Singh S (2016) Carbon nanotube dispersion in nematic liquid crystals: an overview. Prog Mater Sci 80:38–76. https://doi.org/10.1016/j.pmatsci.2015.12.002

Yan L, Chouw N, Jayaraman K (2014) Flax fibre and its composites—a review. Compos Part B Eng 56:296–317. https://doi.org/10.1016/j.compositesb.2013.08.014

Yu T, Ren J, Li S, Yuan H, Li Y (2010) Effect of fiber surface-treatments on the properties of poly(lactic acid)/ramie composites. Compos Part A Appl Sci Manuf 41:499–505. https://doi.org/10.1016/j.compositesa.2009.12.006

Yu B, Jiang Z, Tang X-Z, Yue CY, Yang J (2014) Enhanced interphase between epoxy matrix and carbon fiber with

carbon nanotube-modified silane coating. Compos Sci Technol 99:131–140. https://doi.org/10.1016/j.compscitech.2014.05.021

Zhou F, Cheng G, Jiang B (2014a) Effect of silane treatment on microstructure of sisal fibers. Appl Surf Sci 292:806–812. https://doi.org/10.1016/j.apsusc.2013.12.054

Zhou M, Li Y, He C, Jin T, Wang K, Fu Q (2014b) Interfacial crystallization enhanced interfacial interaction of poly (butylene succinate)/ramie fiber biocomposites using dopamine as a modifier. Compos Sci Technol 91:22–29. https://doi.org/10.1016/j.compscitech.2013.11.019

Publisher's Note Springer Nature remains neutral with regard to jurisdictional claims in published maps and institutional affiliations.